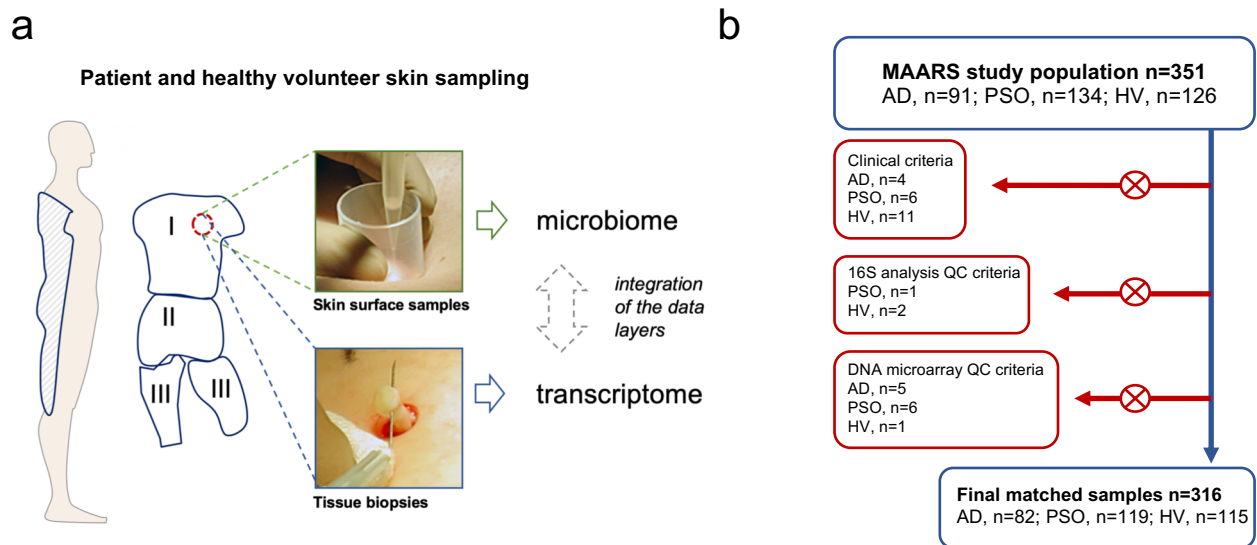


Microbe-host interplay in atopic dermatitis and psoriasis

Fyhrquist *et al*

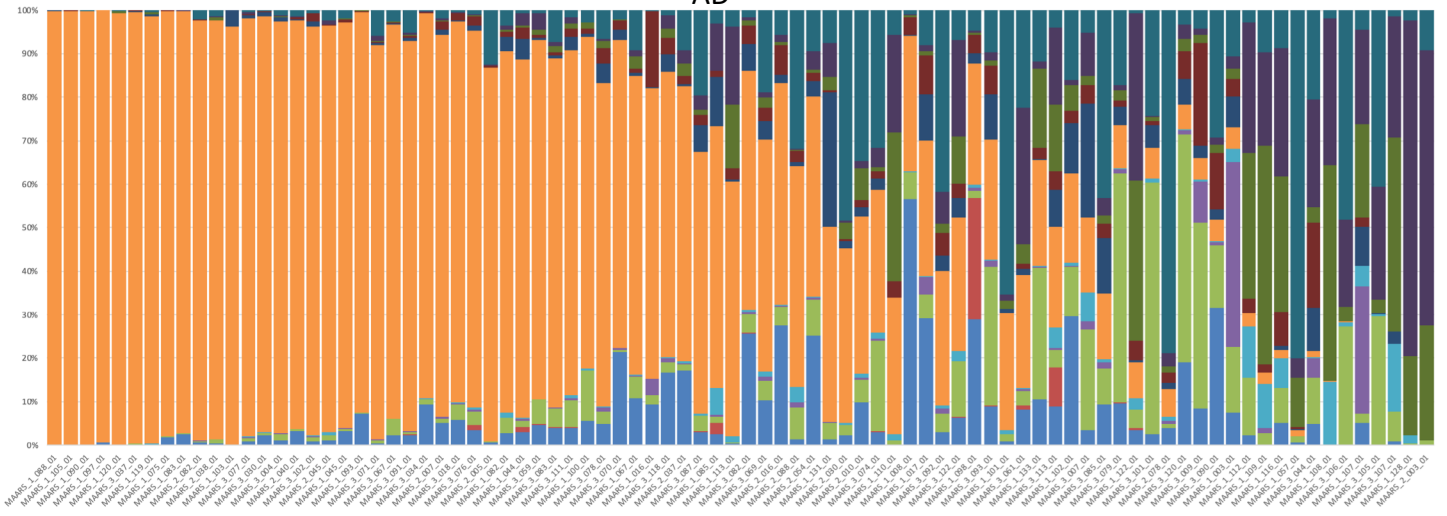


c

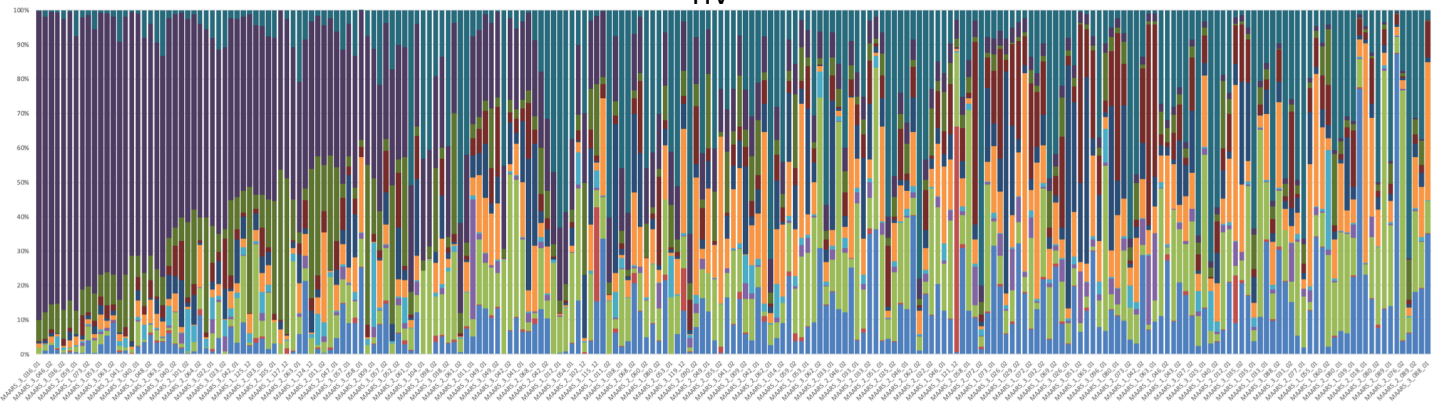
| | Atopic Dermatitis | Psoriasis | Healthy Volunteers |
|----------------|-------------------|------------------|--------------------|
| Numbers | 82 | 119 | 115 |
| Age | | | |
| Mean \pm SEM | 44.49 \pm 1.59 | 48.8 \pm 1.23 | 34.9 \pm 1.17 |
| Range | 20 - 83 | 20 - 77 | 19 - 77 |
| Sex (M/F) | 46/36 | 93/26 | 44/71 |
| SCORAD | 50.6 \pm 1.93 | - | - |
| PASI | - | 14.09 \pm 0.79 | - |

Supplementary Figure 1. Patient sample collection. Patient **a** sampling and **b** enrollment flow chart. **c** Clinical data. The source data files used to generate the present figure are available from the NCBI Sequence Read Archive under accession PRJNA554499, and from EBI ArrayExpress under accession E-MTAB-8149.

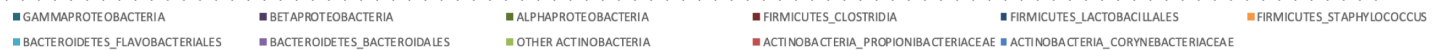
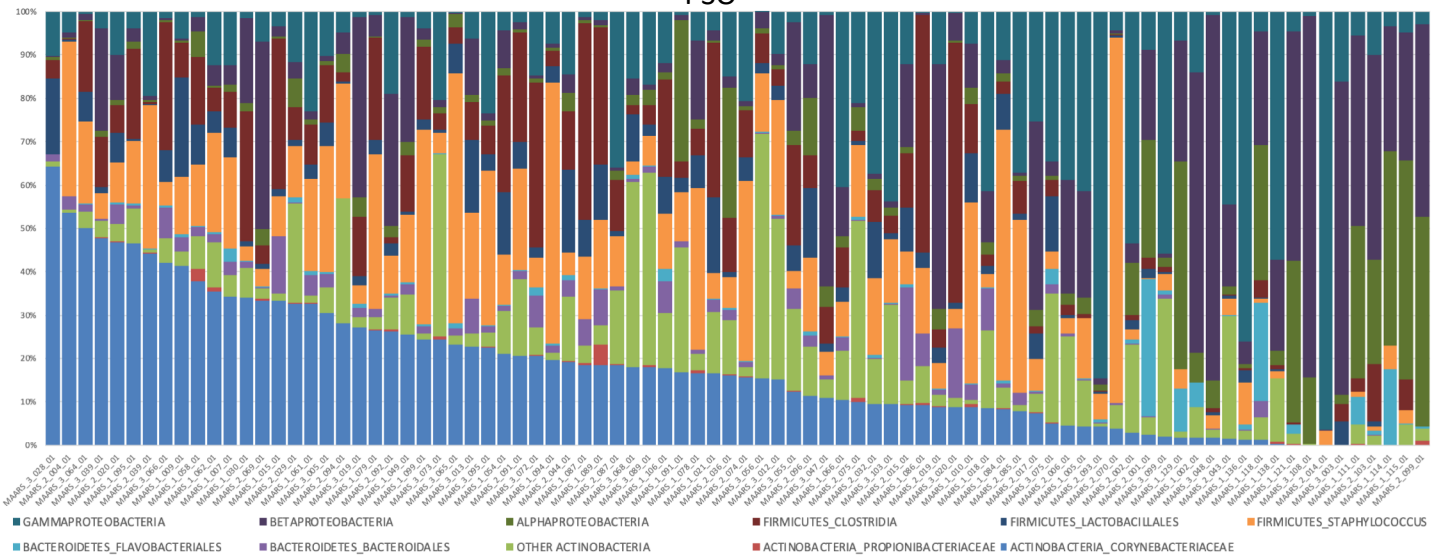
AD



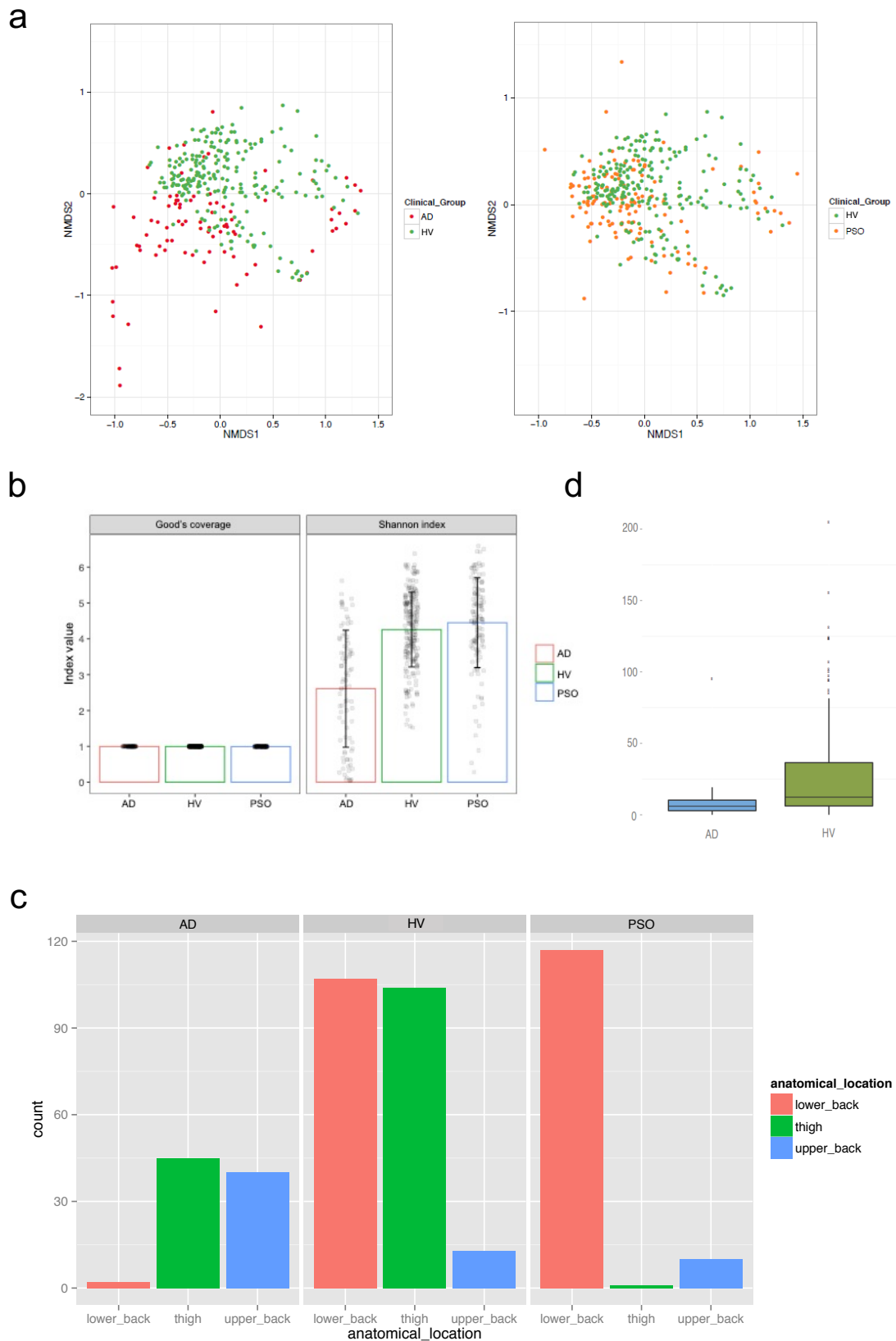
HV



PSO

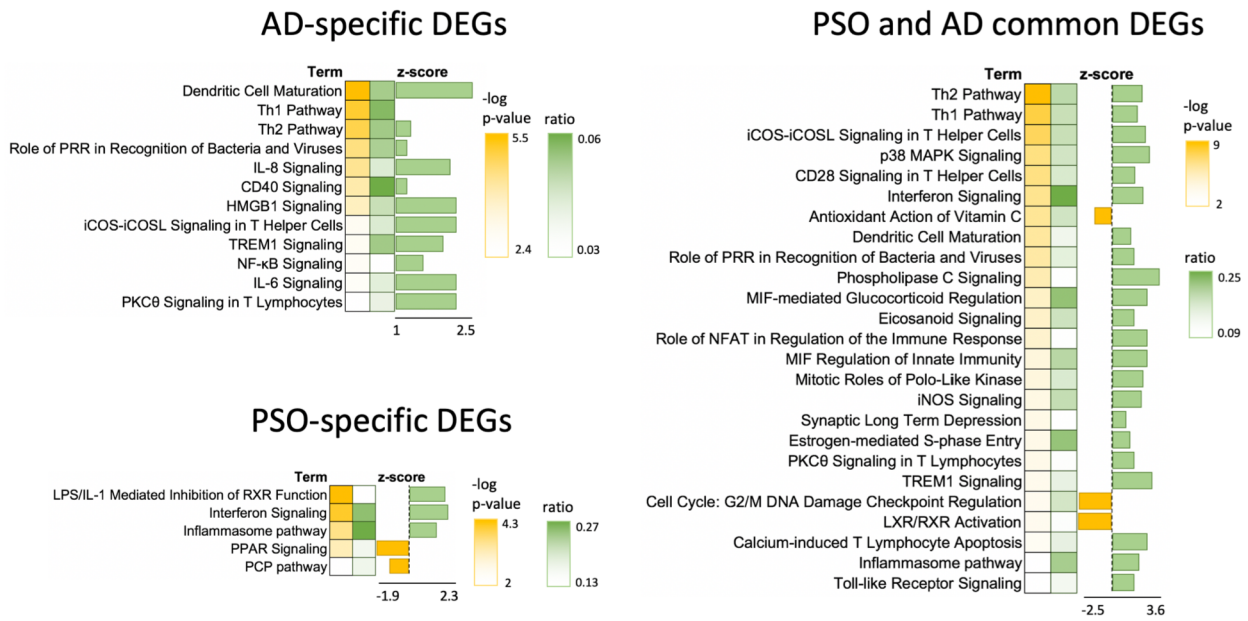


Supplementary Figure 2. Individual compositions of the skin microbiota in AD, HV and PSO. The most abundant bacterial groups depicted for HV, AD and PSO based on 16S rRNA gene sequences. The source data files used to generate the present figure are available from the NCBI Sequence Read Archive under accession PRJNA554499.

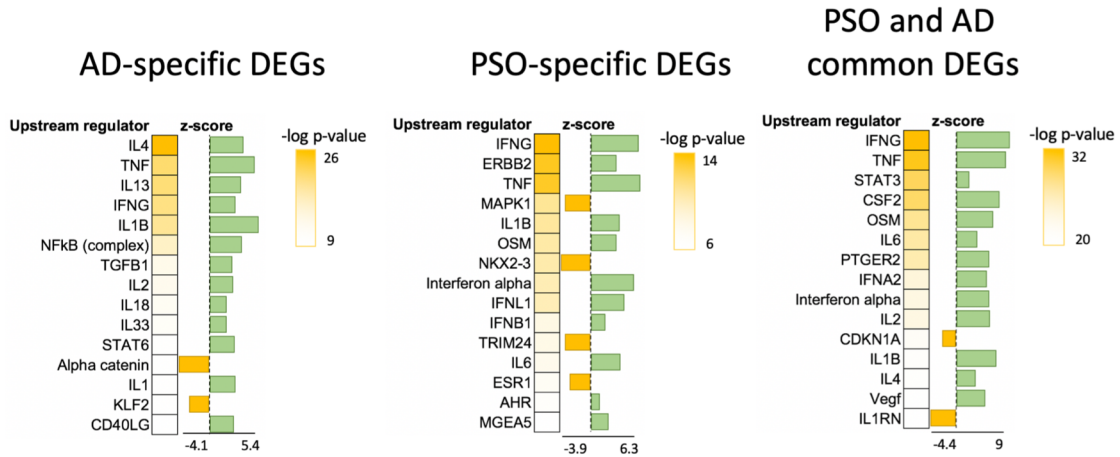


Supplementary Figure 3. Characterization of the skin microbiota in AD and PSO. **a** NMDS analysis of the 95 most abundant OTUs in the three patient groups (HV, $n=115$; AD, $n=82$; PSO, $n=119$). **b** Average Good's coverage and Shannon diversity index in the three sample sets. **c** Sampling from different skin sites in the three different clinical groups, revealing the most significant potential confounding factor. (HV lower back, $n=107$, thigh, $n=104$, upper back, $n=13$; AD, lower back, $n=2$, thigh, $n=44$, upper back, $n=40$; PSO, lower back, $n=107$, thigh, $n=1$, upper back, $n=10$) **d** Anaerobe abundance in AD and HV samples without *S. aureus* (HV, $n=115$, AD, $n=82$, Mann-Whitney U test, p -value 0.0003662) The center line in the boxplots corresponds to the median, the bounding box is the interquartile range (IQR) and the whiskers are defined as 1.5 times IQR. The source data files used to generate the present figure are available from the NCBI Sequence Read Archive under accession PRJNA554499.

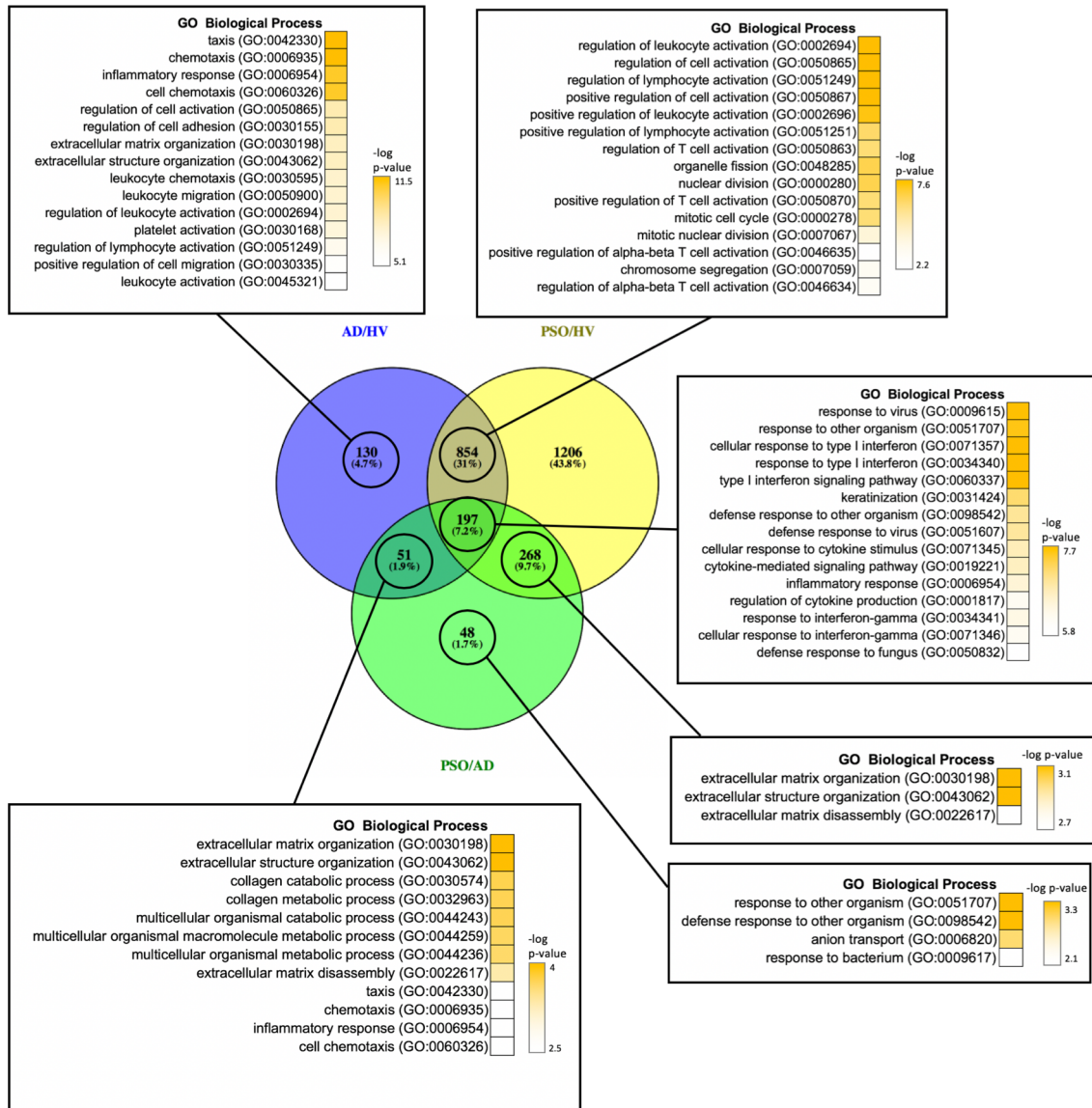
a



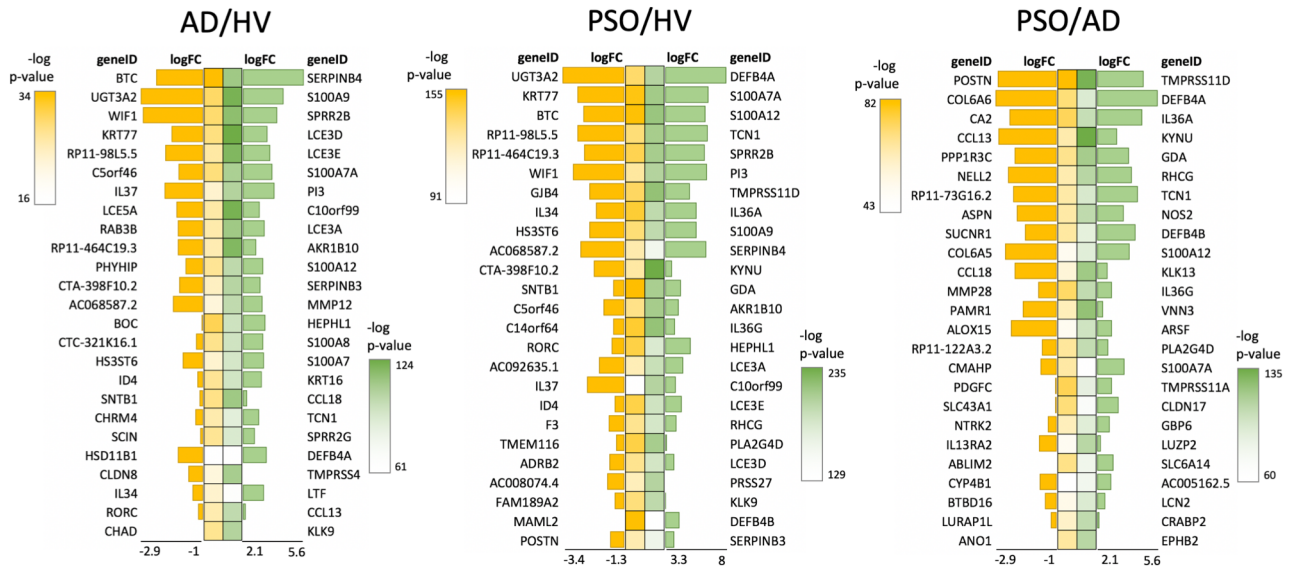
b



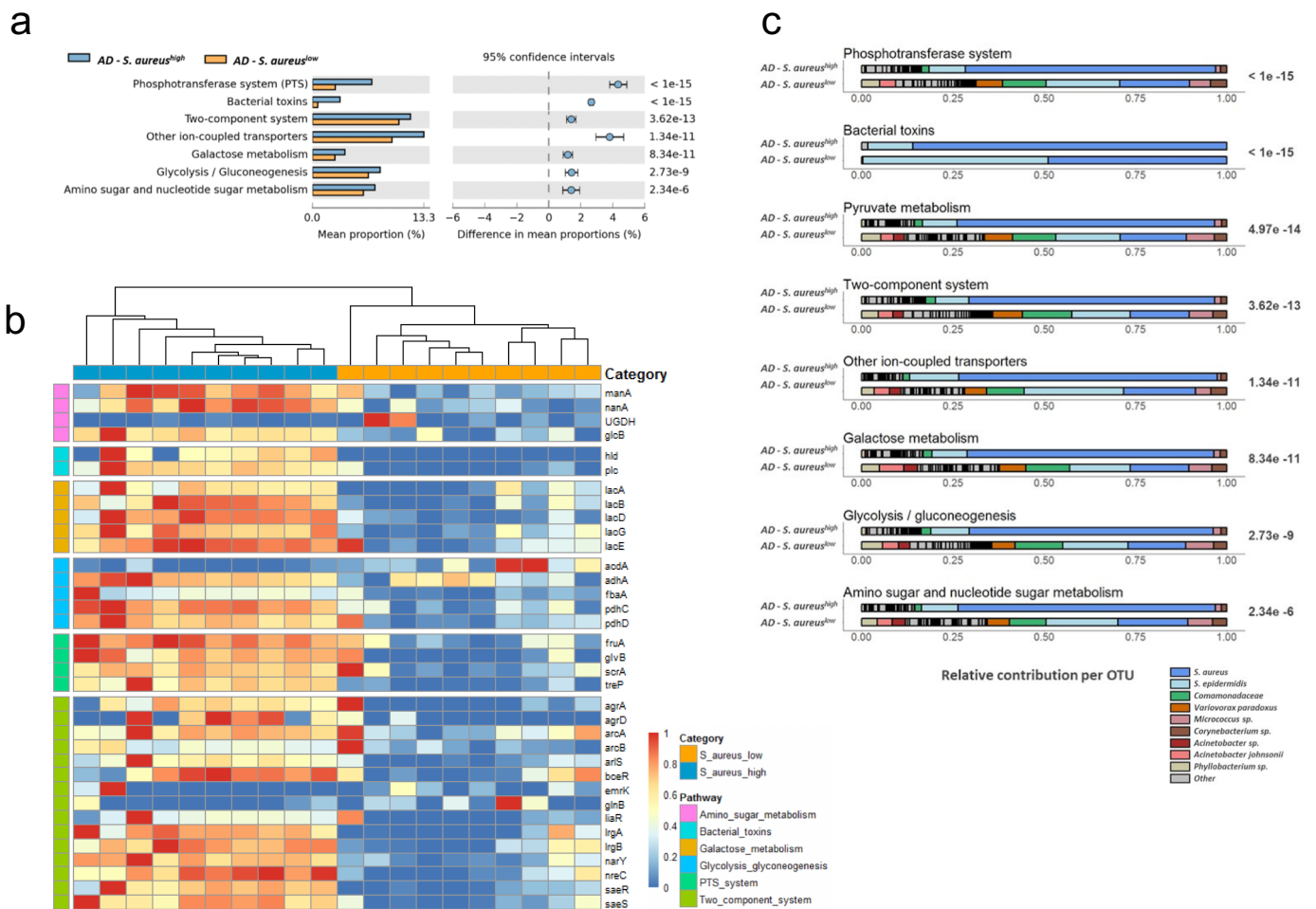
Supplementary Figure 5. The AD and PSO skin transcriptomes. a Most significantly enriched pathways ($-\log p$ -value >2 , z-score >1 or <-1) according to IPA analysis of AD ($n=82$) and PSO ($n=119$) specific and common genes. **b** Top 15 upstream regulators ($-\log p$ -value >2 , z-score >1 or <-1) predicted by IPA. The source data files used to generate the present figure are available from EBI ArrayExpress under accession E-MTAB-8149.



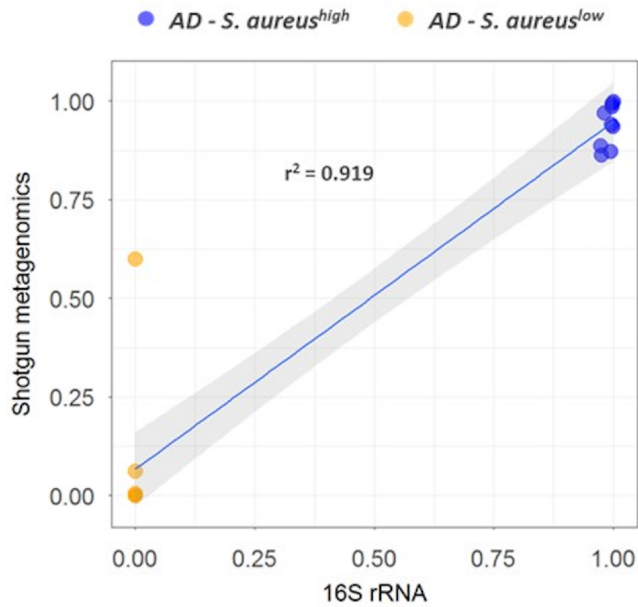
Supplementary Figure 6. Common and distinct functions in AD and PSO skin transcriptomes. GO Term analysis of Venn diagram subsections of AD ($n=82$) and PSO ($n=119$) vs HV ($n=115$) differentially expressed genes; GO Term Biological Process, $-\log p\text{-value} > 2$. The source data files used to generate the present figure are available from EBI ArrayExpress under accession E-MTAB-8149.



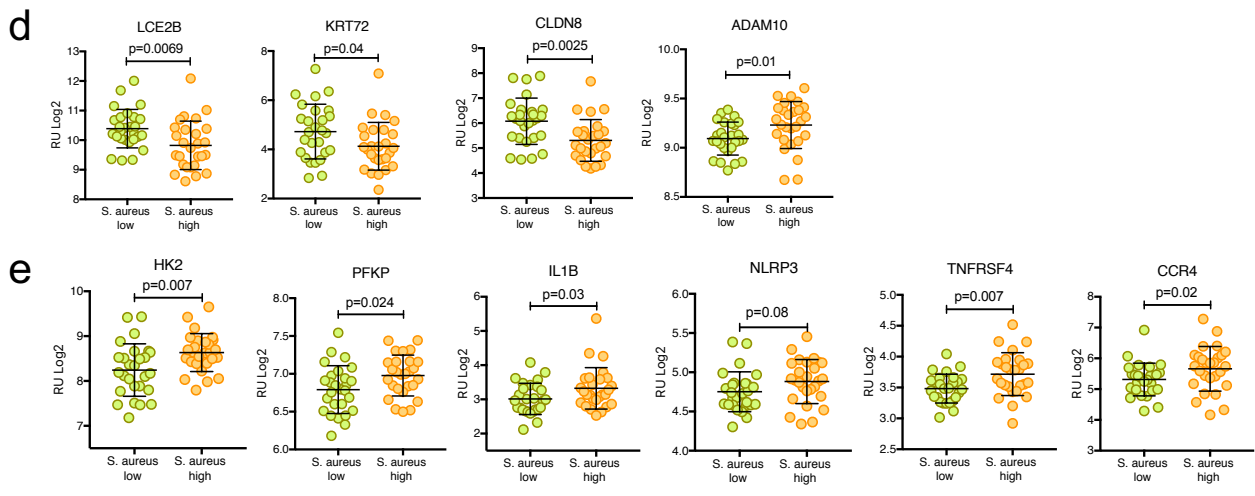
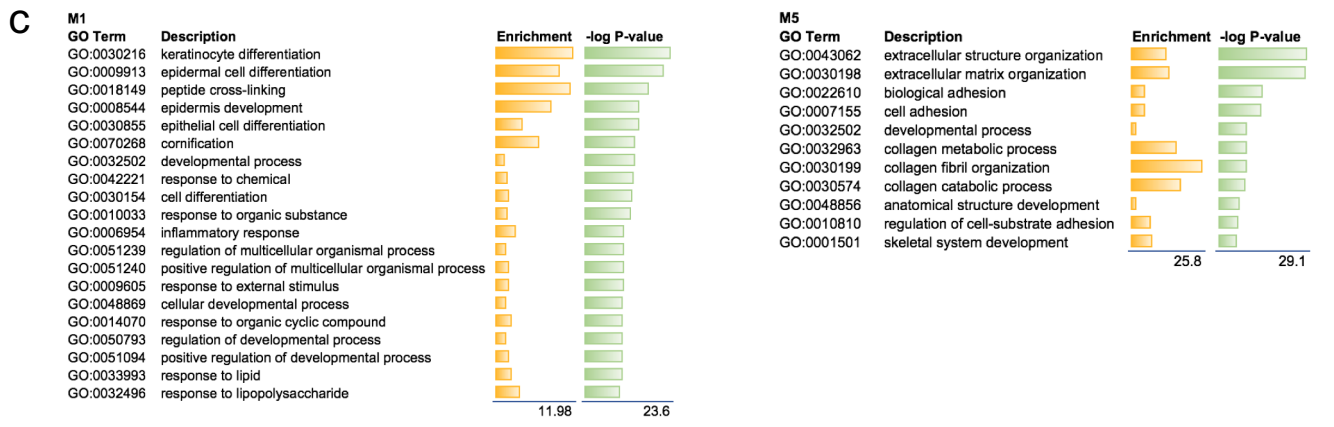
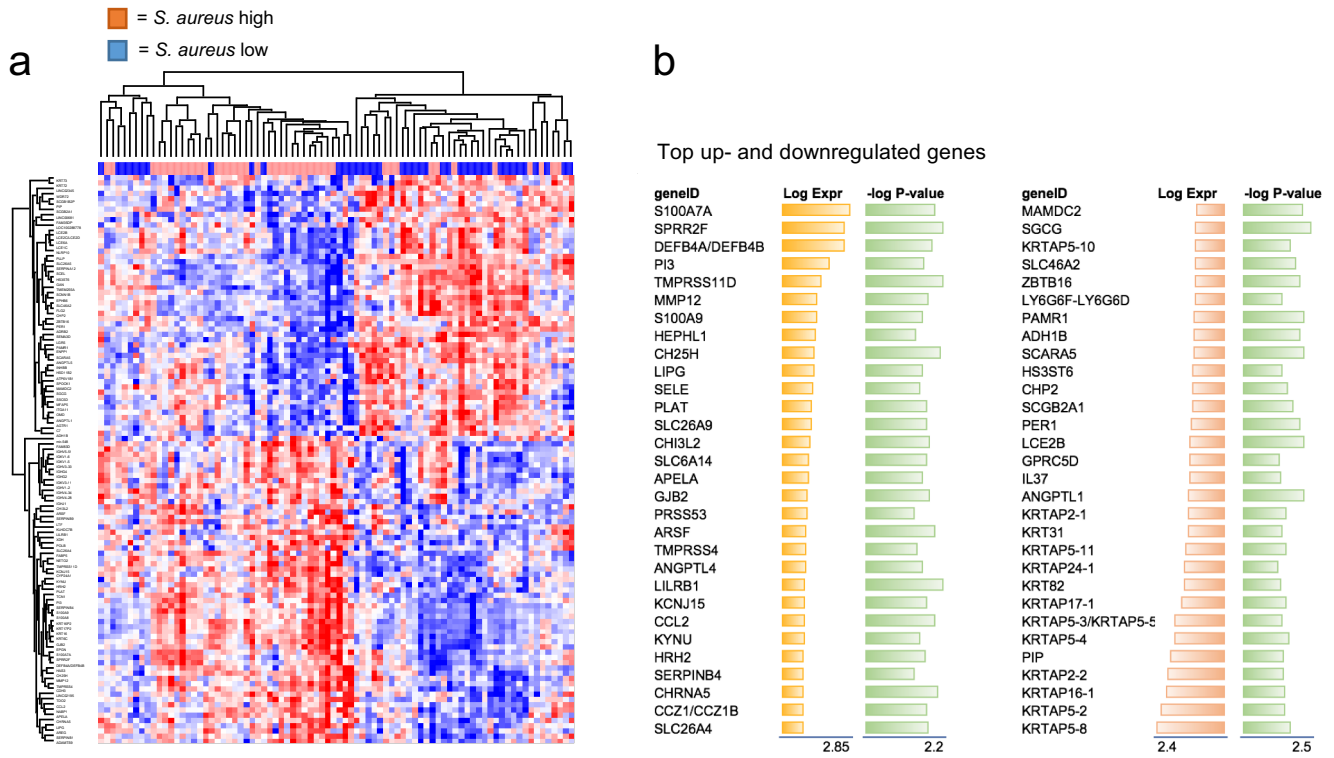
Supplementary Figure 7. Top genes in AD and PSO skin transcriptomes. Top 25 up- and downregulated genes organized according to Rank-value ($-\log p\text{-value} \times \log\text{FC}$). The source data files used to generate the present figure are available from EBI ArrayExpress under accession E-MTAB-8149.



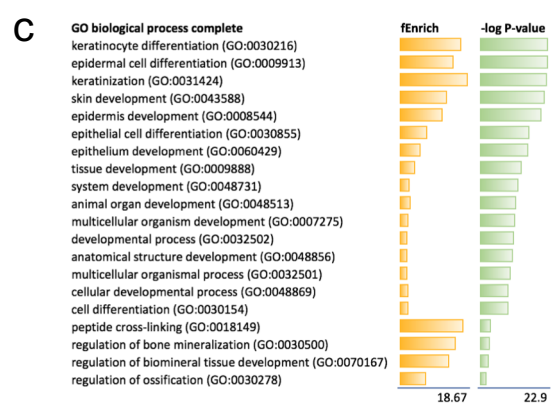
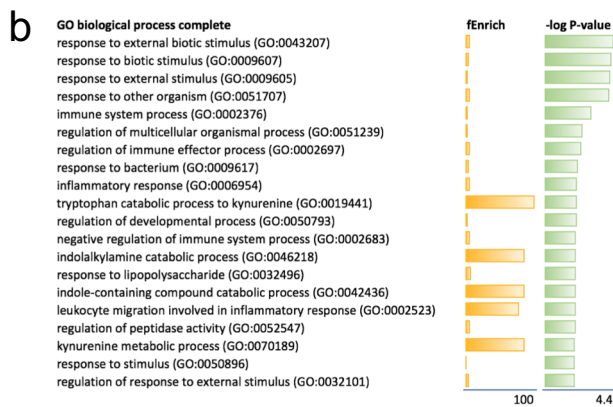
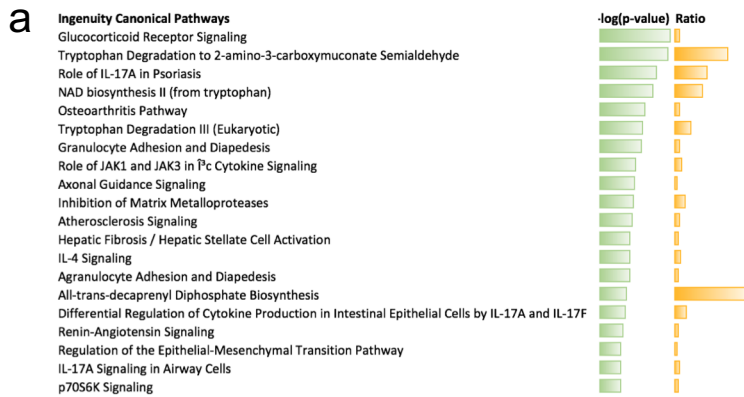
Supplementary Figure 8. Prediction and validation of the *S. aureus* metagenome. **a** Significantly differentially enriched microbial pathways between *S. aureus* 'high' ($n=27$) and 'low' ($n=25$) groups. Gene content of individual OTUs was inferred using the Greengenes v.13.5 database, and subsequently used to predict enriched microbial pathways in the respective disease groups. **b** WGS metagenomic abundances of top differentially abundant genes between *S. aureus* 'high' (blue) and *S. aureus* 'low' (orange) cohorts, annotated by KEGG pathway categories. **c** Contribution of individual OTUs to relevant microbial pathways. The gene content of individual OTUs was inferred using the Greengenes v.13.5 database, and subsequently used to predict enriched microbial pathways in the respective disease groups. Horizontal bars represent the percentage of genes contributed by the most abundant microbes in the dataset. X-axis: sum of relative contributions per sample. Y-axis: contribution across *S. aureus* 'high' and *S. aureus* 'low' samples, respectively. The source data files used to generate the present figure are available from the NCBI Sequence Read Archive under accession PRJNA554499.



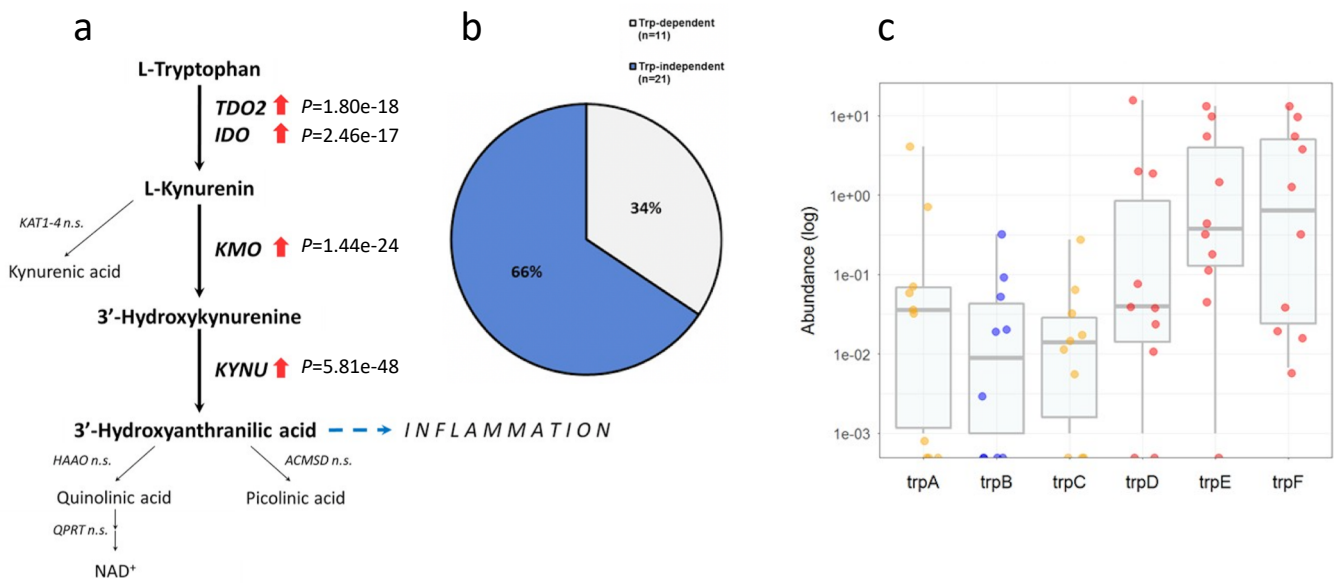
Supplementary Figure 9. Correlation between 16S rRNA gene sequencing and WGS metagenomics data. For validation of 16S OTU classification, preliminary data of WGS metagenomic sequencing of 20 randomly selected samples from 10 *S. aureus* 'high' and 10 *S. aureus* 'low' AD lesions were used. The significant correlation ($r^2=0.919$) shows agreement of taxonomic classification between the independent sequencing methods. The source data files used to generate the present figure are available from the NCBI Sequence Read Archive under accession PRJNA554499.



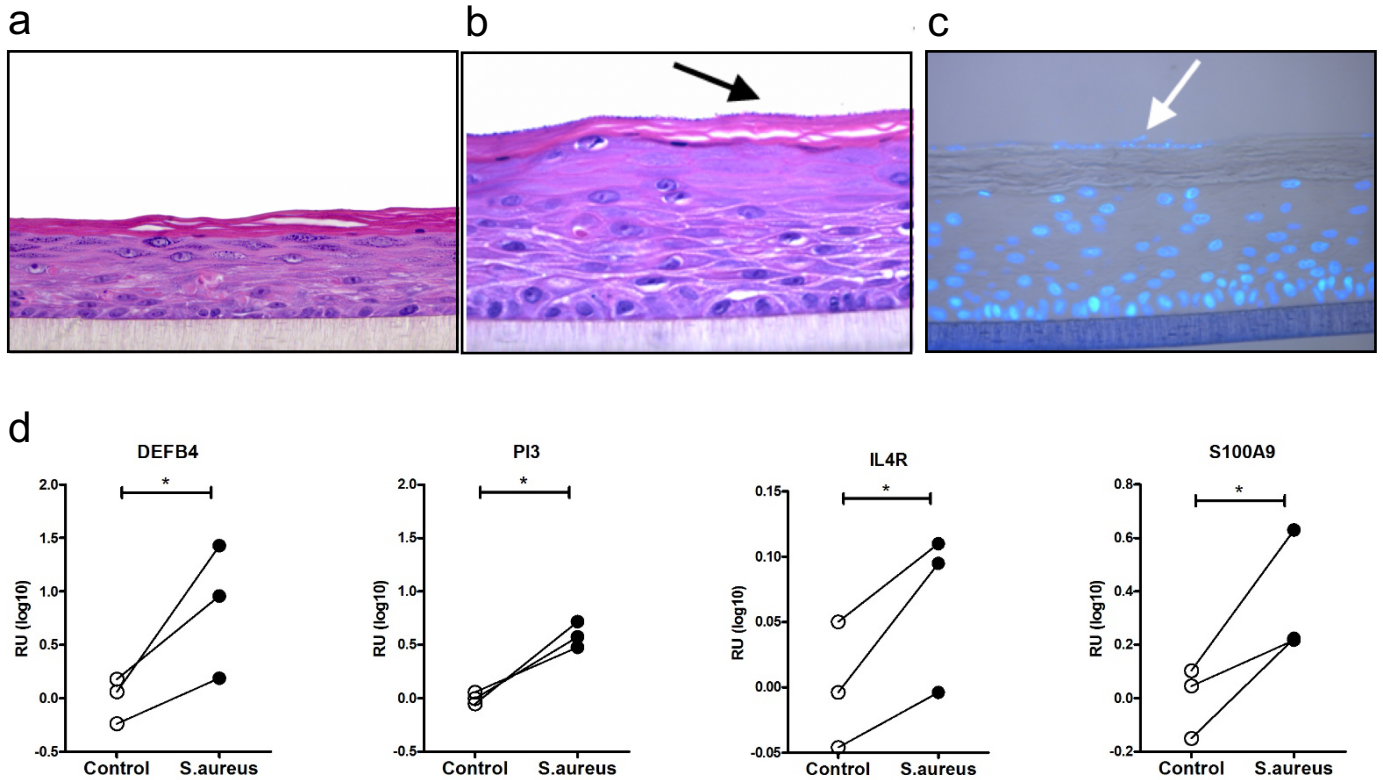
Supplementary Figure 10. Further analysis of the *S. aureus* signature. **a** Hierarchical clustering of differentially expressed host genes between *S. aureus* 'high' ($n=27$) and 'low' ($n=25$) abundance samples (left panel), and **b** a list of top up- and downregulated DEGs. **c** Gene ontology based analysis of biological functions enriched in M1 and M5 modules in the AD gene co-expression network. Statistical analysis (Mann-Whitney U-test) of **d** barrier associated genes, and **e** HIF1A dependent genes, proinflammatory and Th2 type signature genes in *S. aureus* 'high' and 'low' samples. The center line in the dot plots corresponds to the mean, and the error bars to the standard deviation. The source data files used to generate the present figure are available from the NCBI Sequence Read Archive under accession PRJNA554499, and from EBI ArrayExpress under accession E-MTAB-8149.



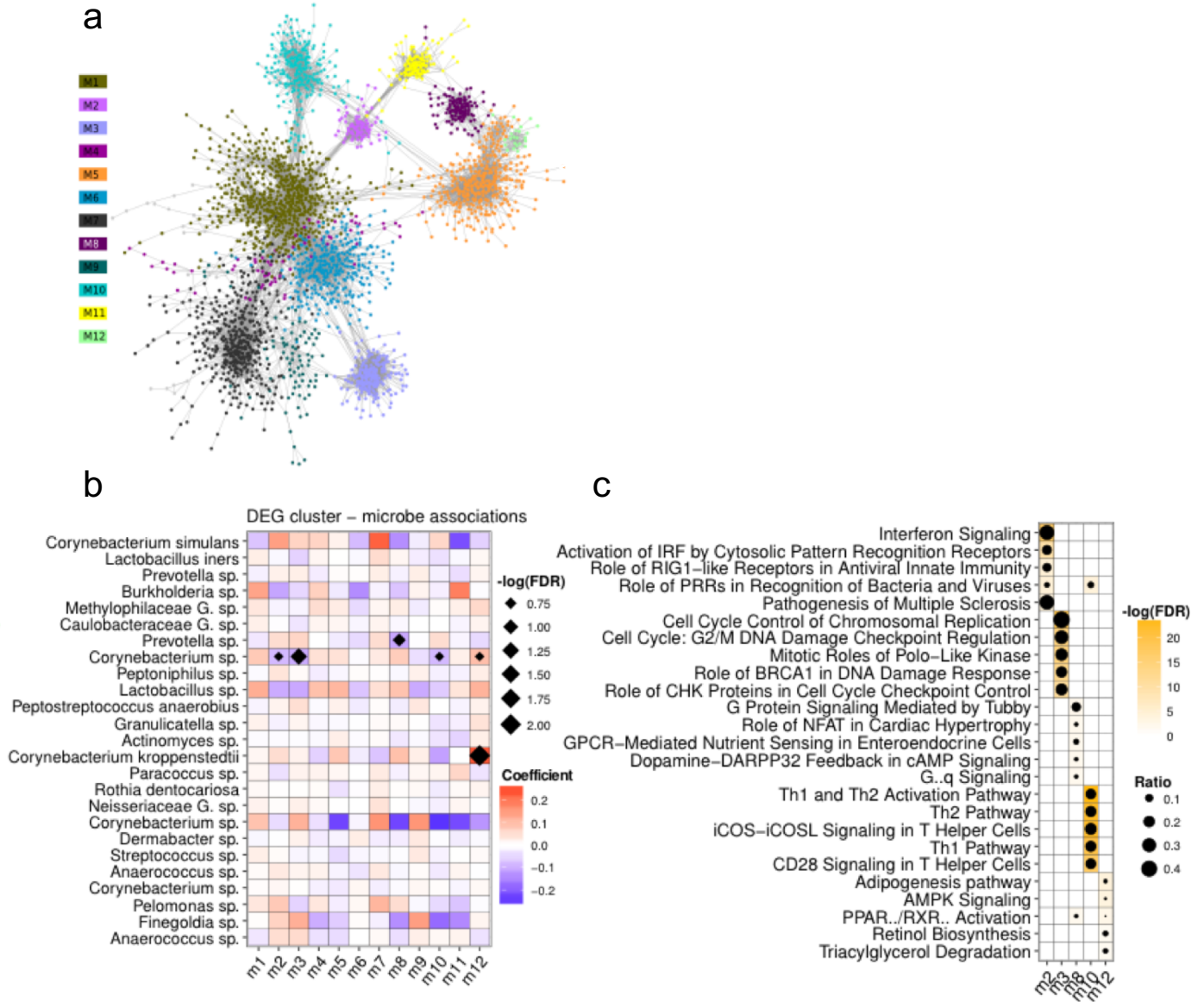
Supplementary Figure 11. Functional enrichment in the *S. aureus* gene signature. **a** Identification of biological function in the *S. aureus* signature (comparing *S. aureus* 'high' ($n=27$) and 'low' ($n=25$) abundance samples), using Ingenuity Pathway analysis (IPA), and **b** Gene ontology based analysis of functional enrichment among up-regulated and **c** down-regulated *S. aureus* signature genes. The source data files used to generate the present figure are available from the NCBI Sequence Read Archive under accession PRJNA554499, and from EBI ArrayExpress under accession E-MTAB-8149.



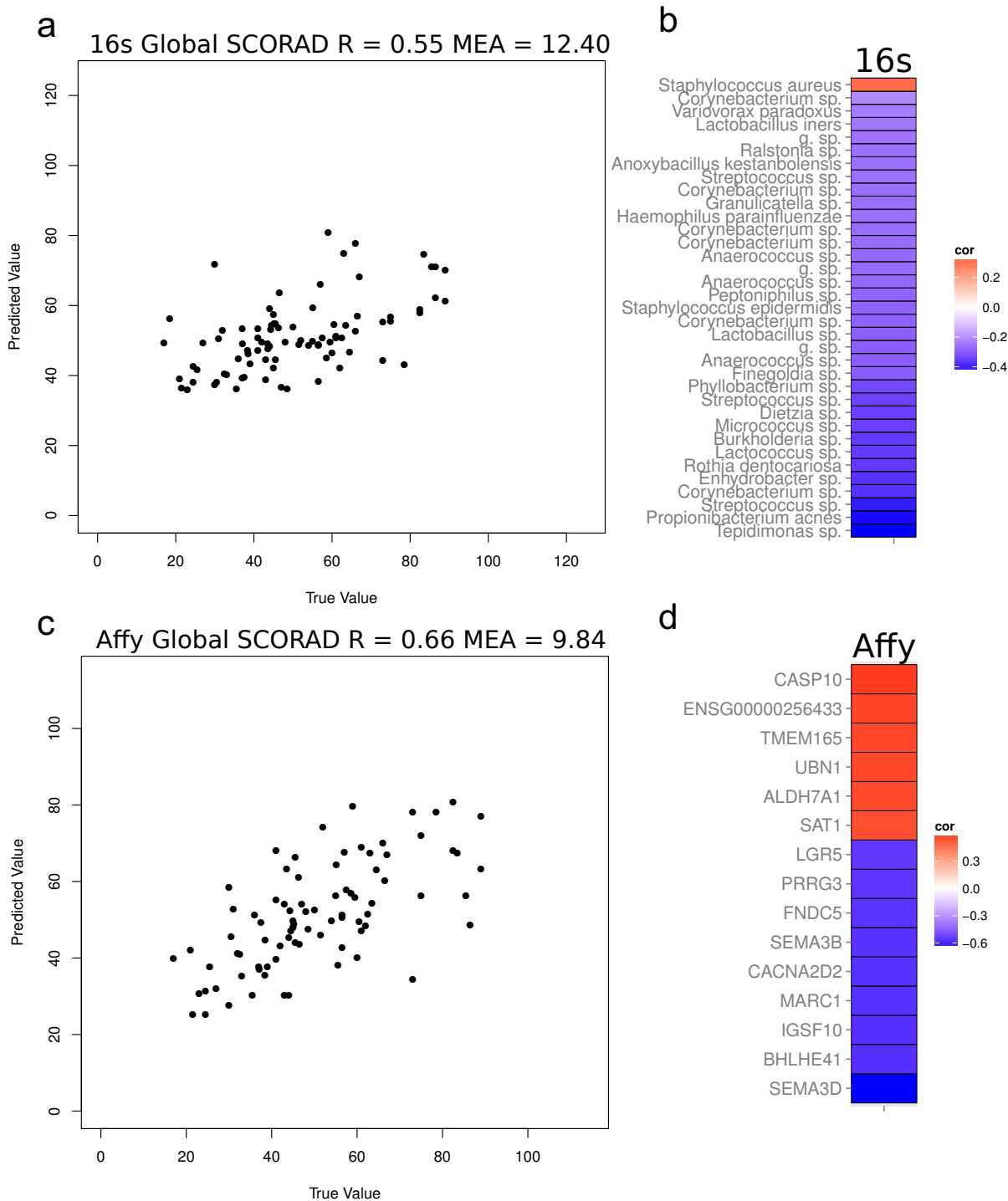
Supplementary Figure 12. Inference of host and microbial functional features. **a** Regulation of the kynureninase pathway of trp degradation on the mRNA level between the *S. aureus* 'high' ($n=27$) and 'low' ($n=25$) cohorts. Red arrows: significantly regulated genes, n.s.: not significant. Arrow and font thickness correspond to significance. **b** Culture-based trp dependence assay of 32 *S. aureus* strains isolated from moderate-to-severe atopic dermatitis patients. Overall, 66% of colonizing *S. aureus* strains were shown to grow independent of trp in trp-depleted culture medium. **c** Presence of tryptophan biosynthesis-related gene families in WGS sequencing results of *S. aureus* 'high' samples. Y axis: relative abundance of UniRef50-defined trp gene families. Boxplots represent the median (center line), interquartile range (hinges) and 1.5x interquartile range (whiskers). The source data files used to generate the present figure are available from the NCBI Sequence Read Archive under accession PRJNA554499, and from EBI ArrayExpress under accession E-MTAB-8149.



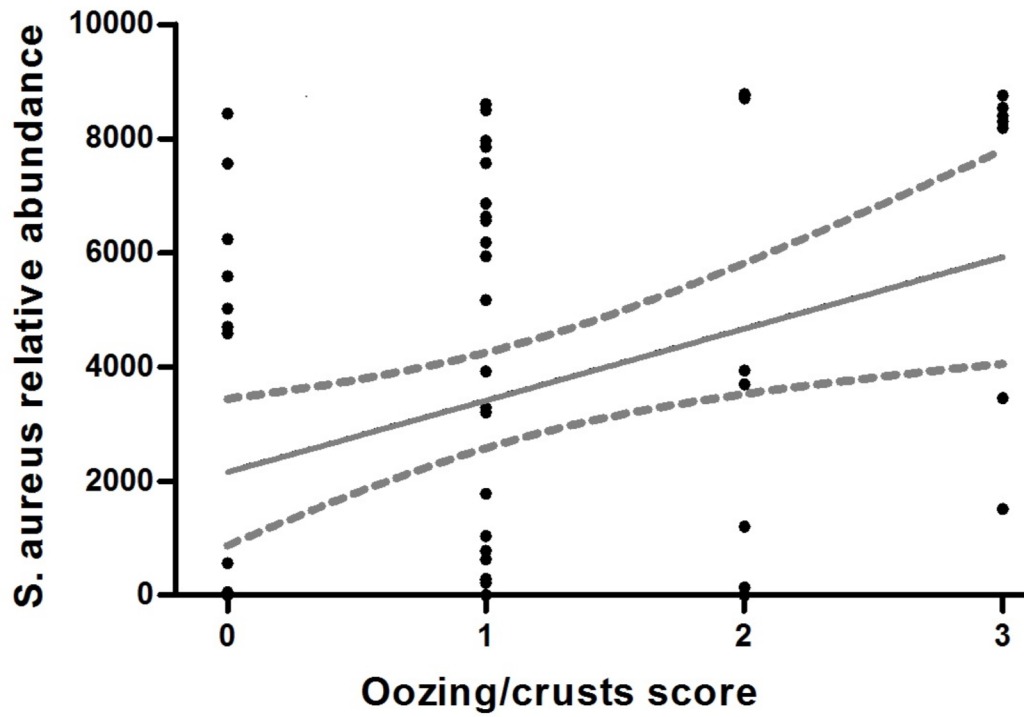
Supplementary Figure 13. Microbial stimulation of human epidermal equivalents (HEEs) **a** Morphological analysis of HEEs. **b** Hematoxylin Eosin (HE) and **c** DAPI staining of microbial colonization of HEEs cultured for 8 days at the air-liquid interface. *S. aureus* bacteria were exposed to the skin equivalent. Arrows indicate visible bacteria on top of the stratum corneum. **d** Statistical analysis ($n=3$, paired one-sided Student's t-test, $p<0.05$) of gene expression after bacterial stimulation; qPCR measurement of selected *S. aureus* signature genes. The source data are provided as a Source Data file.



Supplementary Figure 14. Integrative analysis of PSO microbiome and transcriptome. **a** PSO co-expression network constructed from differentially expressed genes between HV ($n=115$) and PSO ($n=119$) samples resulting in a network of 2653 nodes. The network was partitioned into modules (coloured) using the Louvain method. **b** A linear model was fit for each microbe – module eigengene pair using MaAsLin. The color of heatmap squares correspond to the direction of association and squares correspond to the $-\log(\text{FDR})$ of the association. Associations $\text{FDR} < 0.2$ are shown. **c** Functional analysis of the microbial associated modules conducted using Ingenuity pathway analysis. The heatmap square corresponds to the significance of gene enrichment and the circle indicates the ratio of genes enriched to the total number of genes in the pathway. The source data files used to generate the present figure are available from the NCBI Sequence Read Archive under accession PRJNA554499, and from EBI ArrayExpress under accession E-MTAB-8149.



Supplementary Figure 15. Clinical severity and the AD associated microbiome and transcriptome. The models which achieved the lowest mean absolute error (MAE) are shown. **a** Predicted SCORAD from microbe abundance vs true SCORAD in AD ($n=82$). **b** The 35 selected OTUs included in the regression model. **c** Predicted SCORAD from gene expression vs true SCORAD. **d** The 15 selected genes included in the regression model. The source data files used to generate the present figure are available from the NCBI Sequence Read Archive under accession PRJNA554499, and from EBI ArrayExpress under accession E-MTAB-8149.



Supplementary Figure 16. Association between oozing and abundance of *S. aureus* in AD. Spearman rank-correlation of oozing/crusts clinical scoring and the relative abundance of *S. aureus*. Dashed lines indicate the 95% confidence interval ($r=0.375$, $p=0.002$). The source data files used to generate the present figure are available from the NCBI Sequence Read Archive under accession PRJNA554499, and from EBI ArrayExpress under accession E-MTAB-8149.

Supplementary Table 1. 16S rRNA gene sequencing results.

| OTU | P-value | Statistics | Adjusted P-value | Lowest taxonomic rank |
|------------|----------------------|-------------------|----------------------|------------------------------------|
| OTU883806 | 1.082796337616e-35 | 161.021862716733 | 1.0286565207352e-33 | Staphylococcus aureus (s) |
| OTU912997 | 5.46283956660191e-20 | 88.7074662763379 | 2.59484879413591e-18 | Corynebacterium simulans (s) |
| OTU837884 | 9.03605858513986e-12 | 50.8595960676359 | 2.86141855196096e-10 | Burkholderia (g) |
| OTU1096610 | 2.5332545462453e-11 | 48.7978623299205 | 4.81318363786608e-10 | Finegoldia (g) |
| OTU279980 | 2.47391663531714e-11 | 48.8452668916935 | 4.81318363786608e-10 | Staphylococcus (g) |
| OTU360483 | 9.94086630171859e-11 | 46.0635637059465 | 1.57397049777211e-09 | Neisseriaceae (f) |
| OTU4481323 | 1.25947011945663e-10 | 45.5903196750853 | 1.70928087640542e-09 | Lactobacillus (g) |
| OTU819937 | 3.01928780229458e-10 | 43.8416599068401 | 3.58540426522482e-09 | Caulobacteraceae (f) |
| OTU1107940 | 1.34892167706799e-09 | 40.8479206428008 | 1.42386177023844e-08 | Pelomonas (g) |
| OTU403853 | 7.1974971193661e-09 | 37.4990649873386 | 6.8376222633978e-08 | Propionibacterium acnes (s) |
| OTU4422718 | 8.11527430597365e-09 | 37.2590356684261 | 7.0086459915227e-08 | Corynebacterium kroppenstedtii (s) |
| OTU2110555 | 2.62556441675415e-08 | 34.9107697102301 | 2.07857182993037e-07 | Anaerococcus (g) |
| OTU164003 | 9.11608235073351e-08 | 32.4212811979238 | 6.66175248707449e-07 | Bradyrhizobium (g) |
| OTU851668 | 3.21066791350797e-07 | 29.9032333254332 | 2.17866751273755e-06 | Prevotella (g) |
| OTU285376 | 9.81901229364694e-07 | 27.6675502294912 | 6.21870778597639e-06 | Corynebacterium (g) |
| OTU505749 | 1.27693599311721e-06 | 27.1420942100454 | 7.58180745913343e-06 | Peptoniphilus (g) |
| OTU1131523 | 1.74038585381491e-06 | 26.5228074285116 | 9.7256856367155e-06 | Corynebacterium (g) |
| OTU851925 | 2.17661576395771e-06 | 26.0754785784882 | 1.14876943097504e-05 | Lactobacillus iners (s) |
| OTU370309 | 4.72918068278217e-06 | 24.5235171752701 | 2.36459034139108e-05 | Anaerococcus (g) |
| OTU4047452 | 5.26026525989511e-06 | 24.3106582056967 | 2.3972962332655e-05 | Kocuria palustris (s) |
| OTU4473664 | 5.29928641037868e-06 | 24.2958767720442 | 2.3972962332655e-05 | Peptostreptococcus anaerobius (s) |
| OTU4349859 | 1.08143409972286e-05 | 22.8692748691204 | 4.66982906698509e-05 | Enhydrobacter (g) |
| OTU4317476 | 1.25633952367307e-05 | 22.5694462241174 | 5.18922846734527e-05 | Rothia dentocariosa (s) |
| OTU1003210 | 1.42751891537567e-05 | 22.313975103618 | 5.65059570669537e-05 | Anaerococcus (g) |
| OTU565753 | 1.53247258273243e-05 | 22.1720859337037 | 5.82339581438323e-05 | Corynebacterium (g) |
| OTU4439089 | 2.30010650514732e-05 | 21.3599400730429 | 8.40423530726907e-05 | Actinomyces (g) |
| OTU25478 | 3.25462292613402e-05 | 20.6656980810517 | 0.000114514510363975 | Dermabacter (g) |
| OTU820692 | 4.41632532074884e-05 | 20.0552350287999 | 0.000149839606043264 | Methylophilaceae (f) |
| OTU2901965 | 8.18154204770622e-05 | 18.8220896354653 | 0.000268016032597723 | Streptococcus (g) |
| OTU610043 | 8.72834319123579e-05 | 18.6926997929869 | 0.000276397534389133 | Prevotella (g) |
| OTU4422405 | 0.000158343082584874 | 17.5014929405462 | 0.000485244930502033 | Micrococcus (g) |
| OTU4667218 | 0.000188527688220535 | 17.1525313495029 | 0.000559691574404714 | Ochrobactrum (g) |
| OTU4349522 | 0.000235861283115594 | 16.7045334183191 | 0.000678994602908529 | Anaerococcus (g) |
| OTU4021335 | 0.000358285265261406 | 15.8683621170504 | 0.000972488577138102 | Acinetobacter johnsonii (s) |
| OTU4327300 | 0.000354110582277029 | 15.8918026285942 | 0.000972488577138102 | Anaerococcus (g) |
| OTU4474056 | 0.0003744782030314 | 15.7799522246355 | 0.000988207206355508 | Peptoniphilus (g) |
| OTU4301457 | 0.000394243876987359 | 15.6770817260568 | 0.00101224779226484 | Tepidimonas (g) |
| OTU25259 | 0.000442534685634347 | 15.4459834219479 | 0.00110633671408587 | Streptococcus (g) |
| OTU761594 | 0.000509220645297227 | 15.1652582950573 | 0.00124040926418555 | Thermoanaerobacterium (g) |
| OTU4482598 | 0.00067807366364214 | 14.5925092549719 | 0.00161042495115008 | Acinetobacter (g) |
| OTU496787 | 0.00076154145347984 | 14.3603319009979 | 0.00176454727025817 | Staphylococcus epidermidis (s) |
| OTU4348347 | 0.000801405338649813 | 14.2582873962601 | 0.0018006010078347 | Paracoccus (g) |
| OTU4440643 | 0.00081500887230443 | 14.2246231049509 | 0.0018006010078347 | Corynebacterium (g) |
| OTU4354809 | 0.00130177582451103 | 13.2880518556299 | 0.0027509488298228 | Caulobacteraceae (f) |
| OTU4471315 | 0.00130308102465291 | 13.2860475992325 | 0.0027509488298228 | Granulicatella (g) |
| OTU4327286 | 0.0015061503805283 | 12.9990541427989 | 0.00310639752500409 | Corynebacterium (g) |
| OTU939571 | 0.00164066078125504 | 12.8253124057905 | 0.003316229238707 | Anaerococcus (g) |
| OTU370134 | 0.0018793796083311 | 12.5551618668838 | 0.00371013416722575 | Blautia (g) |
| OTU4473201 | 0.00191364814941118 | 12.5174876656678 | 0.00371013416722575 | Sphingomonadaceae (f) |
| OTU4460228 | 0.0023330185332872 | 12.120941820233 | 0.00443327352132457 | Corynebacterium (g) |
| OTU1081372 | 0.00632547412707488 | 10.1263405727512 | 0.011556154655233 | WAL_1855D (g) |
| OTU20360 | 0.00629722458427567 | 10.1352925696607 | 0.011556154655233 | Corynebacterium (g) |
| OTU114999 | 0.00731884202030772 | 9.83460631493986 | 0.0131186790930044 | Corynebacterium (g) |
| OTU654307 | 0.0076845054354239 | 9.73347239696594 | 0.0135435704006764 | Peptoniphilus (g) |
| OTU912906 | 0.00948918001575288 | 9.31520615035486 | 0.0163904018453913 | Anaerococcus (g) |
| OTU851917 | 0.01185866631957 | 8.98624059456517 | 0.0189757183934985 | Prevotella (g) |
| OTU625320 | 0.0132115829154091 | 8.65332268114129 | 0.0220193048590151 | Peptoniphilus (g) |
| OTU13445 | 0.0134685490608132 | 8.6147960214163 | 0.0220605544961595 | Corynebacterium (g) |
| OTU1004369 | 0.0139576671582279 | 8.54345260924328 | 0.0220996396671941 | Streptococcus (g) |
| OTU4449324 | 0.0137807034987041 | 8.56897192508829 | 0.0220996396671941 | Cloacibacterium (g) |
| OTU4306540 | 0.0151226364554817 | 8.38312510936484 | 0.02351646938865 | Acinetobacter (g) |
| OTU247720 | 0.0167547193535348 | 8.17815061589198 | 0.025672538481582 | Brevibacterium paucivorans (s) |
| OTU995817 | 0.0187009737330081 | 7.95835937038681 | 0.0281998810259646 | Corynebacterium (g) |
| OTU755148 | 0.0199358610373192 | 7.83047021368167 | 0.0291370276699281 | Jan-68 (g) |
| OTU987144 | 0.019880552466783 | 7.8554863195762 | 0.0291370276699281 | Corynebacterium (g) |
| OTU4456068 | 0.0290090109132525 | 7.08029755222659 | 0.0417553944963483 | Variovorax paradoxus (s) |
| OTU378096 | 0.0328340217314866 | 6.83258010650156 | 0.046555702455093 | Acinetobacter (g) |
| OTU74351 | 0.0357143826595617 | 6.66440359142232 | 0.0498950934214464 | Streptophyta (o) |
| OTU4294554 | 0.0400515715065258 | 6.43517473524541 | 0.0551434680162312 | Facklamia (g) |
| OTU4318084 | 0.0409429245853392 | 6.39115253082071 | 0.0555653976515317 | Gemellaceae (f) |
| OTU4476950 | 0.0419542718473155 | 6.34235003874928 | 0.0561359975421827 | Anaerococcus (g) |
| OTU4346894 | 0.0524125952794498 | 5.8972166972209 | 0.0691555076603852 | Phyllobacterium (g) |
| OTU3208510 | 0.0632800781337968 | 5.5203694415844 | 0.0823507866124753 | Brachybacterium conglomeratum (s) |
| OTU14278 | 0.071302751129314 | 5.28164073408482 | 0.0915373156389842 | Peptoniphilus (g) |
| OTU4303697 | 0.0743916983036289 | 5.19682185061858 | 0.0942294845179299 | Acinetobacter (g) |
| OTU4353642 | 0.0786584697969721 | 5.08527993109938 | 0.0983230872462151 | Paracoccus aminovorans (s) |
| OTU4480063 | 0.0853966582885274 | 4.92089661812827 | 0.105359513472859 | Ralstonia (g) |
| OTU103810 | 0.0939155470503113 | 4.73071867236463 | 0.114384320125379 | Janibacter (g) |
| OTU3841245 | 0.113935116931669 | 4.3442528467405 | 0.137010583652008 | Corynebacterium (g) |
| OTU4421536 | 0.119113987340656 | 4.2534873505924 | 0.141447859967029 | Aerococcus (g) |
| OTU4408996 | 0.126264243391992 | 4.13875679648756 | 0.148087692867151 | Anoxybacillus kestanbolensis (s) |
| OTU4349519 | 0.127886327306842 | 4.1132269550875 | 0.148160988953048 | Anaerococcus (g) |
| OTU4350124 | 0.155484883033482 | 3.72241353461464 | 0.177964625158805 | Acinetobacter (g) |
| OTU282360 | 0.187876566645355 | 3.3439401843588 | 0.212479450377223 | Corynebacterium (g) |
| OTU940083 | 0.201340613631936 | 3.20551441989136 | 0.225027744647458 | Corynebacterium (g) |
| OTU511475 | 0.217936652034388 | 3.0471016908397 | 0.240743976084498 | Streptococcus (g) |
| OTU4369229 | 0.220543954300249 | 3.02331652946101 | 0.24082385814395 | Burkholderiales (o) |
| OTU1036883 | 0.275744867799313 | 2.57655846562051 | 0.297679118646985 | Kocuria rhizophila (s) |
| OTU4468125 | 0.34036796441369 | 2.15545596706709 | 0.363314124684607 | Rhodococcus (g) |
| OTU205025 | 0.416205665397651 | 1.75315150583044 | 0.439328202364188 | Chryseobacterium (g) |
| OTU4411187 | 0.428524598501511 | 1.69481427304153 | 0.447360844589489 | Dietzia (g) |
| OTU4309323 | 0.449932623851577 | 1.59731486440384 | 0.464604339846737 | Haemophilus parainfluenzae (s) |
| OTU4446521 | 0.567899838188449 | 1.13162043405689 | 0.580112737934437 | Lactococcus (g) |
| OTU362390 | 0.77102569799755 | 0.520067150476283 | 0.779228099040078 | Corynebacterium (g) |
| OTU4299324 | 0.928857522610018 | 0.147599836669691 | 0.928857522610018 | Streptococcus (g) |

(s)=species, (g)=genus, (f)=family, (o)=order

Statistical analysis (Kruskal-Wallis test, FDR, $p < 0.05$) of the 16S rRNA gene sequencing results. The source data files used to generate the present table are available from the NCBI Sequence Read Archive under accession PRJNA554499.

Supplementary Table 2. Results of the confounder analysis.

Table for AD

| OTU | P-value | confounders | Adjusted P-value | taxname |
|------------|-------------|---------------------------------|------------------|-----------------------------|
| OTU1096610 | 0.000495857 | Institution;anatomical_location | 0.001685915 | <i>Fingoldia</i> spp. |
| OTU13445 | 0.184305984 | CUSTOM_Age | 0.241015517 | <i>Corynebacterium</i> spp. |
| OTU164003 | 1.28E-05 | Institution | 0.000108666 | <i>Bradyrhizobium</i> spp. |
| OTU378096 | 0.775397085 | Institution | 0.823859403 | <i>Acinetobacter</i> spp. |
| OTU4021335 | 0.855576102 | Institution | 0.855576102 | <i>A.johnsonii</i> |
| OTU4349522 | 9.19E-05 | Institution | 0.000496613 | <i>Anaerococcus</i> spp. |
| OTU4354809 | 0.212677095 | Institution | 0.258250758 | <i>Caulobacteraceae</i> |
| OTU4422405 | 0.009189874 | Institution | 0.019528481 | <i>Micrococcus</i> spp. |
| OTU4456068 | 0.00011685 | Institution;anatomical_location | 0.000496613 | <i>V. paradoxus</i> |
| OTU4481323 | 0.001519295 | Gender | 0.003689717 | <i>Lactobacillus</i> spp. |
| OTU4482598 | 0.630874065 | Institution | 0.714990607 | <i>Acinetobacter</i> spp. |
| OTU820692 | 0.03989263 | Institution | 0.075352746 | <i>Methylophilaceae</i> |
| OTU851668 | 0.069680293 | Institution | 0.107687725 | <i>Prevotella</i> sp. |
| OTU851925 | 0.099164356 | Gender;Institution;CUSTOM_Age | 0.140482837 | <i>L. iners</i> |
| OTU883806 | 2.65E-37 | anatomical_location | 4.50E-36 | <i>S. aureus</i> |
| OTU912906 | 0.05409198 | Gender | 0.091956366 | <i>Anaerococcus</i> spp. |
| OTU939571 | 0.00103751 | Institution | 0.002939612 | <i>Anaerococcus</i> spp. |

Table for PSO

| OTU | P-value | confounders | Adjusted P-value | taxname |
|------------|-------------|---------------------------------|------------------|-----------------------------|
| OTU1096610 | 0.000198593 | Institution;anatomical_location | 0.001290854 | <i>Fingoldia</i> spp. |
| OTU164003 | 0.00260733 | Institution | 0.008473823 | <i>Bradyrhizobium</i> spp. |
| OTU285376 | 6.77E-05 | anatomical_location | 0.000880102 | <i>Corynebacterium</i> spp. |
| OTU4327286 | 0.756887546 | Gender | 0.756887546 | <i>Corynebacterium</i> spp. |
| OTU4354809 | 0.335223099 | Institution | 0.396172753 | <i>Caulobacteraceae</i> |
| OTU4422405 | 0.16060262 | Institution | 0.231981562 | <i>Micrococcus</i> spp. |
| OTU4422718 | 0.000600743 | CUSTOM_Age | 0.002603218 | <i>C. kroppenstedtii</i> |
| OTU4439089 | 0.011351491 | Institution | 0.029513877 | <i>Actinomyces</i> spp. |
| OTU4460228 | 0.204028455 | Gender | 0.265236991 | <i>Corynebacterium</i> spp. |
| OTU4481323 | 0.031441572 | Gender | 0.068123407 | <i>Lactobacillus</i> spp. |
| OTU820692 | 0.092479113 | Institution | 0.158389881 | <i>Methylophilaceae</i> |
| OTU851668 | 0.097470696 | Institution | 0.158389881 | <i>Prevotella</i> spp. |
| OTU851925 | 0.579111601 | Gender;Institution;CUSTOM_Age | 0.627370901 | <i>L. iners</i> |

The table shows the *p*-values and adjusted *p*-values after correction for confounding factors, for abundant OTUs that were significantly associated with disease and also significantly associated with a confounded effect. Associations were tested using the Kruskal-Wallis test for body site and institution, the Mann Whitney U test for gender, and Spearman correlation for age. OTUs with an adjusted *p*-value lower than 0.01 retain significance after correction. The source data files used to generate the present tables are available from the NCBI Sequence Read Archive under accession PRJNA554499.

Supplementary Table 3. The *S. aureus* signature.

| ID | Symbol | Expr Log Ratio | Expr p-value | ID | Symbol | Expr Log Ratio | Expr p-value |
|-----------------|---------------|----------------|--------------|-----------------|-------------------|----------------|--------------|
| ENSG00000184330 | S100A7A | 2,851 | 0,0106 | ENSG00000104213 | PDGFRL | -0,583 | 0,0243 |
| ENSG00000244094 | SPRR2F | 2,65 | 0,00643 | ENSG00000151623 | NR3C2 | -0,584 | 0,017 |
| ENSG00000171711 | DEFB4A/DEFB4B | 2,601 | 0,0126 | ENSG00000160862 | AZGP1 | -0,587 | 0,0181 |
| ENSG00000124102 | PI3 | 2,013 | 0,0223 | ENSG00000108231 | LG1 | -0,591 | 0,027 |
| ENSG00000153802 | TMPRSS11D | 1,652 | 0,00643 | ENSG00000113083 | LOX | -0,591 | 0,0462 |
| ENSG00000262406 | MMP12 | 1,484 | 0,0171 | ENSG00000253047 | | -0,592 | 0,0446 |
| ENSG00000163220 | S100A9 | 1,472 | 0,0248 | ENSG00000112796 | ENPP5 | -0,592 | 0,04 |
| ENSG00000181333 | HEPHL1 | 1,454 | 0,038 | ENSG00000151892 | GFRA1 | -0,597 | 0,0213 |
| ENSG00000138135 | CH25H | 1,358 | 0,0077 | ENSG00000268460 | LOC93429 | -0,597 | 0,0284 |
| ENSG00000101670 | LIPG | 1,344 | 0,024 | ENSG00000166770 | ZNF667-AS1 | -0,597 | 0,0237 |
| ENSG00000007908 | SELE | 1,289 | 0,0283 | ENSG00000220483 | SLC25A51P1 | -0,599 | 0,0265 |
| ENSG00000104368 | PLAT | 1,257 | 0,0183 | ENSG00000163331 | DAPL1 | -0,6 | 0,028 |
| ENSG00000174502 | SLC26A9 | 1,234 | 0,0184 | ENSG00000168405 | CMAHP | -0,603 | 0,042 |
| ENSG00000064886 | CHI3L2 | 1,174 | 0,0153 | ENSG00000173926 | MARCH3 | -0,605 | 0,00917 |
| ENSG00000268104 | SLC6A14 | 1,162 | 0,0185 | ENSG00000076716 | GPC4 | -0,606 | 0,019 |
| ENSG00000248329 | APELA | 1,123 | 0,0243 | ENSG00000007306 | CEACAM7 | -0,607 | 0,0287 |
| ENSG00000165474 | GJB2 | 1,087 | 0,016 | ENSG00000189169 | KRTAP10-12 | -0,607 | 0,0482 |
| ENSG00000231027 | | 1,081 | 0,00643 | ENSG00000092607 | TBX15 | -0,609 | 0,0101 |
| ENSG00000151006 | PRSS53 | 1,06 | 0,0418 | ENSG00000257524 | | -0,61 | 0,0444 |
| ENSG00000062096 | ARSF | 1,053 | 0,0107 | ENSG00000143867 | OSR1 | -0,61 | 0,0187 |
| ENSG00000137648 | TMPRSS4 | 1,018 | 0,0357 | ENSG00000187372 | PCDHB13 | -0,614 | 0,0188 |
| ENSG00000167772 | ANGPTL4 | 1,014 | 0,0245 | ENSG00000163710 | PCOLCE2 | -0,614 | 0,0298 |
| ENSG00000104972 | LILRB1 | 0,982 | 0,00643 | ENSG00000168952 | STXBP6 | -0,614 | 0,0139 |
| ENSG00000157551 | KCNJ15 | 0,959 | 0,019 | ENSG00000164920 | OSR2 | -0,615 | 0,0263 |
| ENSG00000108691 | CCL2 | 0,947 | 0,0106 | ENSG00000122707 | RECK | -0,619 | 0,0219 |
| ENSG00000115919 | KYNU | 0,942 | 0,0297 | ENSG00000170549 | IRX1 | -0,622 | 0,0213 |
| ENSG00000113749 | HRH2 | 0,929 | 0,0202 | ENSG00000196734 | LCE1B | -0,627 | 0,0277 |
| ENSG00000206073 | SERPINB4 | 0,927 | 0,043 | ENSG00000184347 | SLIT3 | -0,628 | 0,00894 |
| ENSG00000169684 | CHRNA5 | 0,915 | 0,00918 | ENSG00000070388 | FGF22 | -0,629 | 0,0187 |
| ENSG00000146574 | CCZ1/CCZ1B | 0,913 | 0,0185 | ENSG00000106078 | COBL | -0,635 | 0,0202 |
| ENSG00000091137 | SLC26A4 | 0,894 | 0,017 | ENSG00000170370 | EMX2 | -0,639 | 0,0181 |
| ENSG00000227300 | KRT16P2 | 0,887 | 0,0275 | ENSG00000103319 | EEF2K | -0,643 | 0,0353 |
| ENSG00000158125 | XDH | 0,885 | 0,0119 | ENSG00000095539 | SEMA4G | -0,643 | 0,0398 |
| ENSG00000236481 | LINC02195 | 0,876 | 0,0463 | ENSG00000201134 | | -0,65 | 0,00275 |
| ENSG00000057149 | SERPINB3 | 0,871 | 0,0185 | ENSG00000174514 | MFS4A | -0,653 | 0,0349 |
| ENSG00000151790 | TD02 | 0,857 | 0,00688 | ENSG00000138669 | PRKG2 | -0,654 | 0,0428 |
| ENSG00000173559 | NABP1 | 0,83 | 0,0323 | ENSG00000070601 | FRMPD1 | -0,66 | 0,0183 |
| ENSG00000279277 | | 0,824 | 0,0208 | ENSG00000188624 | IGFL3 | -0,661 | 0,0405 |
| ENSG00000163638 | ADAMTS9 | 0,817 | 0,0202 | ENSG00000165124 | SVEP1 | -0,661 | 0,0388 |
| ENSG00000143546 | S100A8 | 0,814 | 0,0248 | ENSG00000198816 | ZNF358 | -0,666 | 0,00275 |
| ENSG00000172724 | CCL19 | 0,807 | 0,0126 | ENSG00000187173 | LCE2A | -0,668 | 0,0214 |
| ENSG00000149573 | MPZL2 | 0,773 | 0,023 | ENSG00000131831 | RAI2 | -0,668 | 0,00643 |
| ENSG00000225489 | | 0,772 | 0,0294 | ENSG00000231604 | | -0,669 | 0,0187 |
| ENSG00000171208 | NETO2 | 0,765 | 0,039 | ENSG00000133083 | DCLK1 | -0,671 | 0,0147 |
| ENSG00000164687 | FABP5 | 0,763 | 0,0237 | ENSG00000168447 | SCNN1B | -0,673 | 0,00808 |
| ENSG00000211964 | IGHV3-48 | 0,763 | 0,0223 | ENSG00000100234 | TIMP3 | -0,674 | 0,00105 |
| ENSG00000135074 | ADAM19 | 0,757 | 0,0482 | ENSG00000135063 | FAM189A2 | -0,676 | 0,0188 |
| ENSG00000070501 | POLB | 0,755 | 0,0118 | ENSG00000148671 | ADIRF | -0,678 | 0,017 |
| ENSG00000170542 | SERPINB9 | 0,75 | 0,0236 | ENSG00000227051 | C14orf132 | -0,678 | 0,00688 |
| ENSG00000157193 | LRP8 | 0,743 | 0,0144 | ENSG00000006747 | SCIN | -0,678 | 0,0272 |
| ENSG00000184254 | ALDH1A3 | 0,739 | 0,0262 | ENSG00000182898 | TCHHL1 | -0,681 | 0,0245 |
| ENSG00000062038 | CDH3 | 0,738 | 0,0353 | ENSG00000197953 | AADACL2 | -0,682 | 0,00564 |
| ENSG00000268043 | NBPF10 | 0,737 | 0,0397 | ENSG00000176971 | FIBIN | -0,682 | 0,0314 |
| ENSG00000164430 | CGAS | 0,735 | 0,011 | ENSG00000229255 | | -0,685 | 0,0336 |
| ENSG00000271856 | LINC01215 | 0,723 | 0,0159 | ENSG00000198542 | ITGBL1 | -0,687 | 0,0154 |
| ENSG00000189057 | FAM111B | 0,722 | 0,028 | ENSG00000251580 | LINC02482 | -0,687 | 0,028 |
| ENSG00000143839 | REN | 0,713 | 0,0353 | ENSG00000185345 | PRKN | -0,69 | 0,0265 |
| ENSG00000163874 | ZC3H12A | 0,709 | 0,00832 | ENSG00000136155 | SCEL | -0,69 | 0,0265 |
| ENSG00000025708 | TYMP | 0,707 | 0,0352 | ENSG00000115112 | TFCP2L1 | -0,692 | 0,00808 |
| ENSG00000019186 | CYP24A1 | 0,7 | 0,0299 | ENSG00000254835 | RNF185-AS1 | -0,694 | 0,0259 |
| ENSG00000232445 | | 0,691 | 0,0416 | ENSG00000157514 | TSC22D3 | -0,695 | 0,00643 |
| ENSG00000111801 | BTN3A3 | 0,673 | 0,0135 | ENSG00000189320 | FAM180A | -0,7 | 0,00643 |
| ENSG00000256433 | | 0,668 | 0,0151 | ENSG00000125845 | BMP2 | -0,701 | 0,0398 |
| ENSG00000062716 | VMP1 | 0,661 | 0,0314 | ENSG00000204789 | ZNF204P | -0,701 | 0,0192 |
| ENSG00000105835 | NAMPT | 0,655 | 0,016 | ENSG00000203786 | KPRP | -0,704 | 0,019 |
| ENSG00000117009 | KMO | 0,653 | 0,0208 | ENSG00000198854 | C1orf68 | -0,705 | 0,0229 |
| ENSG00000148459 | PDSS1 | 0,65 | 0,0248 | ENSG00000188783 | PRELP | -0,707 | 0,011 |
| ENSG00000155380 | SLC16A1 | 0,648 | 0,0385 | ENSG00000185940 | KRTAP5-3/KRTAP5-5 | -0,712 | 0,0495 |
| ENSG00000251402 | FAM90A25P | 0,641 | 0,0119 | ENSG00000184564 | SLITRK6 | -0,712 | 0,0282 |
| ENSG00000184731 | FAM110C | 0,633 | 0,0474 | ENSG00000122674 | CCZ1/CCZ1B | -0,713 | 0,0277 |
| ENSG00000188681 | TEKT4P2 | 0,633 | 0,0314 | ENSG00000125355 | TMEM255A | -0,716 | 0,0337 |
| ENSG00000103522 | IL21R | 0,625 | 0,0181 | ENSG00000168477 | TNXB | -0,719 | 0,00653 |
| ENSG00000105639 | JAK3 | 0,624 | 0,0171 | ENSG00000170962 | PDGFD | -0,72 | 0,0181 |
| ENSG00000077238 | IL4R | 0,622 | 0,04 | ENSG00000239521 | GATS | -0,723 | 0,00643 |
| ENSG00000145287 | PLAC8 | 0,62 | 0,0184 | ENSG00000248290 | TNXA | -0,726 | 0,0424 |
| ENSG00000119714 | GPR68 | 0,616 | 0,0245 | ENSG00000000005 | TNMD | -0,728 | 0,0243 |
| ENSG00000030110 | BAK1 | 0,615 | 0,0106 | ENSG00000201608 | RNU4-42P | -0,729 | 0,0246 |
| ENSG00000097046 | CD7C | 0,614 | 0,0219 | ENSG00000152377 | SPOCK1 | -0,732 | 0,0146 |
| ENSG00000160766 | GBAP1 | 0,605 | 0,0467 | ENSG00000169252 | ADRB2 | -0,733 | 0,0104 |
| ENSG00000151014 | NOCT | 0,601 | 0,0457 | ENSG00000186207 | LCE5A | -0,736 | 0,00841 |
| ENSG00000021355 | SERPINB1 | 0,598 | 0,0445 | ENSG00000232220 | | -0,739 | 0,0184 |
| ENSG00000119630 | PGF | 0,593 | 0,00806 | ENSG00000183287 | CCBE1 | -0,739 | 0,0213 |
| ENSG00000042062 | RIPOR3 | 0,591 | 0,0159 | ENSG00000184022 | OR2T10 | -0,739 | 0,0314 |
| ENSG00000196584 | XRCC2 | 0,587 | 0,011 | ENSG00000102934 | PLLP | -0,741 | 0,0183 |
| ENSG00000258689 | LINC01269 | 0,585 | 0,0495 | ENSG00000114771 | AADAC | -0,743 | 0,0126 |
| ENSG00000155189 | AGPAT5 | 0,584 | 0,0243 | ENSG00000189014 | FAM35DP | -0,744 | 0,0487 |

For identification of differentially expressed genes between *S. aureus* 'high' and 'low' samples, a linear model (R package Limma) was fitted to the data, and pairwise comparisons were done using the empirical Bayes method. Transcriptomes were defined based on a fold change of 1.5 or greater and a Benjamini-Hochberg adjusted *p*-value less than 0.05. The source data files used to generate the present table are available from the NCBI Sequence Read Archive under accession PRJNA554499, and from EBI ArrayExpress under accession E-MTAB-8149.

Supplementary Table 3, continued...

| ID | Symbol | Expr Log Ratio | Expr p-value |
|-----------------|-------------------|----------------|--------------|
| ENSG00000205221 | VIT | -0,745 | 0,0104 |
| ENSG00000105143 | SLC1A6 | -0,746 | 0,00643 |
| ENSG00000170381 | SEMA3E | -0,748 | 0,0181 |
| ENSG00000172201 | ID4 | -0,751 | 0,0304 |
| ENSG00000176387 | HSD11B2 | -0,754 | 0,0168 |
| ENSG00000214783 | POLR2J4 | -0,754 | 0,00643 |
| ENSG00000203392 | | -0,758 | 0,0193 |
| ENSG00000119138 | KLF9 | -0,761 | 0,00841 |
| ENSG00000178776 | C5orf46 | -0,771 | 0,0276 |
| ENSG00000187170 | LCE4A | -0,774 | 0,0251 |
| ENSG00000106123 | EPHB6 | -0,777 | 0,0145 |
| ENSG00000143412 | ANXA9 | -0,778 | 0,0387 |
| ENSG00000249731 | | -0,78 | 0,0402 |
| ENSG00000165953 | SERPINA12 | -0,786 | 0,0438 |
| ENSG00000259225 | LINC02345 | -0,789 | 0,00887 |
| ENSG00000144891 | AGTR1 | -0,791 | 0,0118 |
| ENSG00000234477 | | -0,796 | 0,00688 |
| ENSG00000185950 | IRS2 | -0,797 | 0,00643 |
| ENSG00000153930 | ANKFN1 | -0,8 | 0,0306 |
| ENSG0000011341 | MGP | -0,8 | 0,00311 |
| ENSG00000179954 | SSC5D | -0,805 | 0,00678 |
| ENSG00000212658 | KRTAP29-1 | -0,835 | 0,0448 |
| ENSG00000261609 | GAN | -0,84 | 0,0331 |
| ENSG00000205864 | KRTAP5-6 | -0,844 | 0,0304 |
| ENSG00000153993 | SEMA3D | -0,846 | 0,00982 |
| ENSG00000163145 | C1QTNF7 | -0,853 | 0,00345 |
| ENSG00000163083 | INHBB | -0,853 | 0,00275 |
| ENSG00000166415 | WDR72 | -0,859 | 0,0341 |
| ENSG00000187223 | LCE2C/LCE2D | -0,86 | 0,0243 |
| ENSG00000197614 | MFAP5 | -0,866 | 0,00841 |
| ENSG00000221305 | mir-548 | -0,871 | 0,0349 |
| ENSG00000137809 | ITGA11 | -0,881 | 0,00643 |
| ENSG00000212900 | KRTAP3-2 | -0,883 | 0,0149 |
| ENSG00000235942 | LCE6A | -0,883 | 0,023 |
| ENSG00000244411 | KRTAP5-7 | -0,901 | 0,0287 |
| ENSG00000186393 | KRT26 | -0,919 | 0,0261 |
| ENSG00000196859 | KRT39 | -0,919 | 0,0405 |
| ENSG00000269729 | | -0,928 | 0,0324 |
| ENSG00000143520 | FLG2 | -0,933 | 0,0192 |
| ENSG00000127083 | OMD | -0,943 | 0,0185 |
| ENSG00000116678 | LEPR | -0,951 | 0,0337 |
| ENSG00000156284 | CLDN8 | -0,967 | 0,0288 |
| ENSG00000186049 | KRT73 | -0,975 | 0,028 |
| ENSG00000279301 | OR2T11 | -0,975 | 0,0243 |
| ENSG00000170615 | SLC26A5 | -0,977 | 0,00366 |
| ENSG00000197594 | ENPP1 | -0,982 | 0,00345 |
| ENSG00000131686 | CA6 | -0,988 | 0,023 |
| ENSG00000170486 | KRT72 | -0,992 | 0,039 |
| ENSG00000116039 | ATP6V1B1 | -0,996 | 0,0139 |
| ENSG00000197084 | LCE1C | -1,012 | 0,00643 |
| ENSG00000187151 | ANGPTL5 | -1,016 | 0,023 |
| ENSG00000139292 | LGR5 | -1,021 | 0,046 |
| ENSG00000165072 | MAMDC2 | -1,025 | 0,00678 |
| ENSG00000102683 | SGCG | -1,042 | 0,00345 |
| ENSG00000204572 | KRTAP5-10 | -1,046 | 0,0183 |
| ENSG00000119457 | SLC46A2 | -1,051 | 0,0118 |
| ENSG00000109906 | ZBTB16 | -1,055 | 0,00808 |
| ENSG00000250641 | LY6G6F-LY6G6D | -1,061 | 0,0392 |
| ENSG00000149090 | PAMR1 | -1,092 | 0,00643 |
| ENSG00000196616 | ADH1B | -1,127 | 0,0083 |
| ENSG00000168079 | SCARA5 | -1,135 | 0,00638 |
| ENSG00000162040 | HS3ST6 | -1,148 | 0,0355 |
| ENSG00000166869 | CHP2 | -1,161 | 0,0248 |
| ENSG00000124939 | SCGB2A1 | -1,166 | 0,0146 |
| ENSG00000179094 | PER1 | -1,189 | 0,00841 |
| ENSG00000232324 | | -1,218 | 0,000241 |
| ENSG00000159455 | LCE2B | -1,241 | 0,00643 |
| ENSG00000226005 | | -1,243 | 0,0199 |
| ENSG00000111291 | GPRC5D | -1,25 | 0,0456 |
| ENSG00000125571 | IL37 | -1,257 | 0,0406 |
| ENSG00000116194 | ANGPTL1 | -1,285 | 0,00643 |
| ENSG00000212725 | KRTAP2-1 | -1,306 | 0,028 |
| ENSG00000094796 | KRT31 | -1,326 | 0,0388 |
| ENSG00000204571 | KRTAP5-11 | -1,407 | 0,028 |
| ENSG00000188694 | KRTAP24-1 | -1,438 | 0,0498 |
| ENSG00000161850 | KRT82 | -1,447 | 0,0413 |
| ENSG00000186860 | KRTAP17-1 | -1,537 | 0,0275 |
| ENSG00000196224 | KRTAP5-3/KRTAP5-5 | -1,787 | 0,0377 |
| ENSG00000241598 | KRTAP5-4 | -1,8 | 0,0202 |
| ENSG00000159763 | PIP | -1,922 | 0,0341 |
| ENSG00000214518 | KRTAP2-2 | -2,052 | 0,0326 |
| ENSG00000212657 | KRTAP16-1 | -2,067 | 0,029 |
| ENSG00000205867 | KRTAP5-2 | -2,277 | 0,0304 |
| ENSG00000241233 | KRTAP5-8 | -2,422 | 0,0189 |

Supplementary Table 4. Tryptophan dependence of AD associated *S. aureus* strains.

| S. aureus strains | Trp dependence | |
|-------------------|--------------------|--------------------|
| | NO | YES |
| Donor #1 | | x |
| Donor #2 | | x |
| Donor #3 | | x |
| Donor #4 | x | |
| Donor #5 | x | |
| Donor #6 | | x |
| Donor #7 | x | |
| Donor #8 | x | |
| Donor #9 | x | |
| Donor #10 | x | |
| Donor #11 | | x |
| Donor #12 | x | |
| Donor #13 | | x |
| Donor #14 | x | |
| Donor #15 | x | |
| Donor #16 | x | |
| Donor #17 | x | |
| Donor #18 | x | |
| Donor #19 | x | |
| Donor #20 | x | |
| Donor #21 | x | |
| Donor #22 | x | |
| Donor #23 | x | |
| Donor #24 | | x |
| Donor #25 | | x |
| Donor #26 | x | |
| Donor #27 | | x |
| Donor #28 | x | |
| Donor #29 | x | |
| Donor #30 | x | |
| Donor #31 | | x |
| Donor #32 | | x |
| Σ | 66% (21/32) | 34% (11/32) |

Supplementary Table 5. Primers used in the study.

| Primers used in the study | | | | | | |
|--|----------------------------|-------------------------|----------------|-------------------------|------------------|-------|
| Gene expression analysis of 3d human epidermal equivalents (HEEs) | | | | | | |
| Hugo Gene Symbol | Forward primer 5'>3' | Reverse primer 5'>3' | cDNA specific | Slope | E fold | E % |
| DEFB4 | gatgcctcctccagggtttt | ggatgacatatggctccactct | yes | -3.36 | 1.99 | 99.3 |
| PI3 | catgagggccagcagctt | tttaacagggaactcccgtgaca | yes | -3.3 | 2.02 | 100.9 |
| IL4R | ctgcctgttgctatgctc | tctgatcccaccattcttct | yes | -3.16 | 2.1 | 105.2 |
| S100A8 | ccgagtgctcctcagtatatcaggaa | acgcccatctttatcaccagaat | yes | -3.36 | 1.98 | 99.2 |
| 16S rRNA gene sequencing | | | | | | |
| Forward primer | Sequence | Adaptors | Reverse primer | Sequence | Adaptors | |
| 341f | 5'-CCTACGGGNGGCWGCAG | adptor B, Lib-L | 805r | 5'-GACTACHVGGTATCTAATCC | adaptor A, Lib-L | |